Separation Science and Technology
Publication details, including instructions for authors and subscription information:
http://www.informaworld.com/smpp/title~content=t713708471

Effect of Coalescence on the Performance of a Continuous Foam Fractionation Column

Farooq Uraizee[a]; Ganesan Narsimhan[a]
[a] DEPARTMENT OF AGRICULTURAL ENGINEERING, PURDUE UNIVERSITY, WEST LAFAYETTE, INDIANA

To cite this Article Uraizee, Farooq and Narsimhan, Ganesan(1992) 'Effect of Coalescence on the Performance of a Continuous Foam Fractionation Column', Separation Science and Technology, 27: 7, 937 — 953
To link to this Article: DOI: 10.1080/01496399208019734
URL: http://dx.doi.org/10.1080/01496399208019734

SEPARATION SCIENCE AND TECHNOLOGY, **27**(7), pp. 937–953, 1992

Effect of Coalescence on the Performance of a Continuous Foam Fractionation Column

FAROOQ URAIZEE and GANESAN NARSIMHAN*
DEPARTMENT OF AGRICULTURAL ENGINEERING
PURDUE UNIVERSITY
WEST LAFAYETTE, INDIANA 47907

Abstract

A model for the hydrodynamics of coalescing foam bed is proposed which accounts for liquid drainage through thin films and plateau borders, bubble coalescence, and mixing of liquid between thin films and plateau borders. Foam bed is assumed to consist of equal sized dodecahedral bubbles at any cross section, and the variation of bubble size with foam height due to coalescence is described through phenomenological models. This model is employed to investigate the effect of coalescence on enrichment and recovery for the nonanol–water system in a continuous foam fractionation column for different inlet bubble sizes, superficial gas velocities, and inlet concentrations. Coalescence is found to yield higher enrichments and lower recoveries, possibly because of the predominant effect of increased liquid drainage due to larger bubble sizes resulting in a significant decrease in liquid holdup with foam height. Larger bubble sizes and lower superficial gas velocities were found to result in higher enrichments and lower recoveries. There exists an optimum inlet concentration for which enrichment was found to be maximum. Enrichment was found to be highest for coalescence frequency proportional to the surface area of bubbles, intermediate for frequency proportional to the bubble size, and lowest for constant coalescence frequency.

INTRODUCTION

Foam fractionation is an adsorptive bubble separation technique based on the selective adsorption of one or more surface-active solutes at the gas–liquid interface. Understanding the interplay among various phenomena such as liquid drainage in thin films and plateau borders, coalescence of bubbles, and interbubble gas diffusion is necessary for the prediction of separation efficiency in foam fractionation columns. There have been many attempts to model the hydrodynamics of foam beds. Detailed reviews of

*To whom correspondence should be addressed.

foam fractionation and its process application can be found (*1–4*). Many investigators have accounted for the effects of (a) gravity drainage from plateau borders (*5–7*), (b) drainage of liquid from the plateau borders as well as from thin films (*5*, *8*), (c) surface viscosity (*9–13*), and (d) interbubble gas diffusion (*14*, *15*) in their calculation of foam densities. Coalescence due to rupture of thin films as a result of van der Waals mediated growth of imposed thermal perturbation has been incorporated into the hydrodynamics of foam beds in order to predict the collapse of foam (*13*). The effects of (a) bubble size distribution, (b) coalescence due to rupture of thin films, and (c) interbubble gas diffusion have been accounted for in a comprehensive population balance model (*15*). Previous models for a semibatch foam fractionation column have recently been extended to the prediction of enrichment and recovery in a continuous foam fractionation column (*16*). Prediction of coalescence frequencies from stability analysis of thin films to imposed perturbations is rendered difficult due to the inability to characterize mechanical perturbations ever present in a foam column. Consequently, coalescence frequencies may be better described by phenomenological models characterized by the measurements of bubble size.

In this paper we propose a model for the hydrodynamics of a coalescing foam bed. The foam bed is assumed to consist of dodecahedral bubbles of the same size at any cross section. The variation of bubble size with foam height due to coalescence is described through phenomenological models for coalescence frequency. Partial mixing of the liquid in thin films and plateau borders due to internal reflux resulting from coalescence is accounted for. This model was employed to investigate the effect of coalescence on enrichment and recovery for nonanol–water system in a continuous foam fractionation column. The salient features of the model are described in the next section. The subsequent section discusses the effect of coalescence on enrichment and recovery for different inlet bubble sizes, superficial gas velocities, and inlet concentrations.

HYDRODYNAMICS OF COALESCING FOAM BED

In a continuous foam fractionation column, an inert gas is bubbled through a liquid pool whose holdup is maintained constant by introducing feed to the liquid pool and withdrawing the bottom product from the liquid pool. Upon reaching the top of the liquid pool, inert gas bubbles form a foam (stabilized by surfactant adsorbed at the gas–liquid interface) which moves up the column, entraining some liquid from the pool. The foam consists of polyhedral bubbles, and the entrained liquid is distributed between thin films and plateau borders. Liquid from thin film drains into the adjacent plateau borders under the action of plateau border suction and disjoining pressure whereas liquid in the interconnected network of plateau borders drains under the action of gravity. Rupture of draining thin liquid films due to the growth of imposed thermal and mechanical perturbations leads to coalescence of bubbles. When a thin film ruptures, the surfactant in the bulk as well as adsorbed surfactant from the destroyed interface will be redistributed between the plateau borders and thin films. This internal reflux of surfactant due to coalescence leads to enrichment of surfactant in the bulk which, in turn, may lead to more adsorption at the gas–liquid interface. Even though the concentration of surfactant in the plateau borders and films will be the same at the foam–liquid interface, subsequent enrichments in plateau borders and thin films may be different depending on the manner in which the liquid in the destroyed thin film is distributed between thin films and plateau borders. If the internal reflux is distributed uniformly into films and plateau borders, the surfactant concentrations will be the same in both, i.e., the liquid is well mixed. On the other hand, if the internal ieflux is distributed only into the plateau borders, the surfactant concentration in the films will not change, i.e., the films and plateau borders are segregated. The real situation will lie between the above two extremes. The film concentration c_f can be related to plateau border concentration c_p through

$$c_f = c_b + m(c_p - c_b) \tag{1}$$

where c_b is the pool concentration and m is the phenomenological mixing parameter. When m is unity, the surfactant concentration is the same in thin films and plateau borders. When m is zero, on the other hand, the system is segregated and the film concentration is always equal to the pool concentration.

Two important measures of performance of a continuous foam fractionation column for the concentration of a surfactant are enrichment and recovery. Enrichment e is defined as

$$e = c_T/c_F \tag{2}$$

where c_T and c_F refer to the top product and feed concentrations, respectively. Recovery r is defined as

$$r = \frac{c_T T}{c_F F} = e\frac{T}{F} \tag{3}$$

where T and F refer to the flow rates of top product and feed, respectively. In order to predict enrichment and recovery, one should have knowledge of liquid holdup and total amount of surfactant in the top product. Liquid holdup profile can be obtained by solving balance equations for liquid in films and plateau borders. The surface concentration of surfactant can be assumed to be in equilibrium with the bulk and therefore can be evaluated from the adsorption isotherm. Several simplifying assumptions are employed in the model. The foam is assumed to consist of dodecahedral bubbles. Bubble size at any cross section of the foam bed is assumed to be uniform. Coalescence is accounted for by allowing the bubble size to vary with foam height even though, as pointed out earlier, bubbles at any height are of the same size. Such an assumption is likely to be valid only for narrow bubble size distributions and therefore for sufficiently small coalescence rates since coalescence tends to broaden bubble size distribution. The foam is assumed to move in plug flow, and the plateau borders are assumed to be randomly oriented. If N is the number of bubbles per unit volume of the foam and η is the number of bubbles entrained per unit area of cross section of the foam, we have

$$\frac{d\eta}{dz} = -\frac{N}{2}\beta \tag{4}$$

where z is the distance along the foam column from the foam–liquid interface and β, the coalescence frequency, is the fraction of bubbles collapsing per unit time. β and N can be related to the superficial gas velocity G, bubble volume V_b [$= (4\pi/3)R^3$, R being the equivalent bubble radius], and liquid holdup ϵ through

$$\eta = \frac{G}{V_b}, \qquad N = \frac{1 - \epsilon}{V_b} \tag{5}$$

Combining Eqs. (4) and (5):

$$\frac{dR}{dz} = \frac{\beta(1 - \epsilon)R}{6G} \tag{6}$$

Material balance of liquid in thin films yields

$$\frac{-d}{dz}(\eta n_f A_f x_f) - N n_f A_f V - \frac{N}{2} n_f A_f x_f \beta = 0 \tag{7}$$

where n_f is the number of films per bubble, A_f is the area of film, x_f is the film thickness, and V is the velocity of film drainage. In the above equation, the first term represents the change in the volume of liquid in film due to convection, the second term represents flow of liquid from the films, and the third term represents the loss of liquid due to rupture of thin films.

Balance of liquid in plateau borders yields

$$-\frac{d}{dz}(\eta n_p a_p l) + \frac{d}{dz}\left(\frac{4}{15}N n_p a_p u R\right) + N n_f A_f V + \frac{N}{2}\beta n_f A_f x_f = 0 \quad (8)$$

where n_p is the number of plateau borders per bubble, a_p is the area of cross section of plateau border, l is the length of plateau border, R is the bubble radius, and u is the velocity of gravity drainage. In the above equation, the first term refers to the change in the liquid due to convection, the second term refers to the change due to gravity drainage, the third term refers to the drainage of liquid from thin films to plateau borders, and the last term refers to the internal reflux of liquid from ruptured thin films.

A material balance for surfactant in the foam yields

$$-\frac{d}{dz}(\eta n_p a_p l c_p + \eta n_f A_f x_f c_f + \eta n_f A_f \Gamma) + \frac{d}{dz}\left(\frac{4}{15}N n_p u R c_p\right) = 0 \quad (9)$$

where c_p and c_f refer to the surfactant concentrations in the plateau borders and thin films, respectively, which are related via Eq. (1). In the above equation, Γ is the surface concentration of surfactant, in equilibrium with the bulk film concentration c_f, which can be evaluated from the adsorption isotherm. Equations (6), (7), (8), and (9) have to be solved in conjunction with Eq. (1) with appropriate boundary conditions at the foam–liquid interface, to be discussed later, in order to obtain R, x_f, a_p, c_p, and c_f as a function of foam height. Of course, knowledge of velocity of film drainage V, gravity drainage of plateau border u, and adsorption isotherm of surfactant are necessary for solving the above equations. Enrichment and recovery can then be calculated from

$$\epsilon = N n_f A_f x_f + N n_p a_p l \quad (10)$$

$$e = \frac{(N n_f A_f x_f c_f + N n_p a_p l c_p + N n_f A_f \Gamma)_T}{c_F \epsilon_T} \quad (11)$$

and

$$r = \frac{(\eta n_f A_f x_f c_f + \eta n_p a_p l c_p + \eta n_f A_f \Gamma)_T}{F c_F} \tag{12}$$

where ϵ_T refers to the liquid holdup at the top of the column, F is the feed flow rate per unit cross-sectional area of the foam column, and $(\ldots)_T$ refers to the evaluation of the quantity within the parentheses at the top of the foam column.

For an immobile gas–liquid interface, the velocity of film drainage V can be evaluated from Reynolds equation,

$$V = \frac{2}{3} \frac{\Delta p x_f^3}{\mu R_F^2} \tag{13}$$

where R_F is the radius of the film, μ is the viscosity, and Δp is the pressure drop due to plateau border suction responsible for flow, given by

$$\Delta p = \sigma / R_p \tag{14}$$

In the above equation, σ is the surface tension and R_p is the radius of curvature of plateau border. The surface tension σ is, in turn, given by

$$\sigma = \sigma_0 - \Pi \tag{15}$$

where σ_0 is the surface tension of pure gas–liquid interface and Π is the surface pressure of gas–liquid interface due to the adsorption of surfactant. From geometric considerations (*9*), the radius of curvature of plateau border R_p can be related to x_f and a_p to yield

$$R_p = \frac{-1.732 x_f + \{(1.732 x_f)^2 - 0.644(0.433 x_f^2 - a_p)\}^{1/2}}{0.322} \tag{16}$$

When the gas–liquid interface is mobile, the velocity of film drainage will be higher than that predicted by Reynold's equation. Appropriate equations for film drainage accounting for interfacial mobility in terms of surface viscosity, surface diffusions, and diffusion of surfactant from the bulk can be found elsewhere (*17*). In the present calculations, the gas–liquid interface is assumed to be immobile so that Eq. (13) can be employed.

The velocity of gravity drainage through plateau border for immobile gas–liquid interface is given by (*18*),

$$u = \frac{\rho g a_p}{20\sqrt{3}\mu} \tag{17}$$

where ρ is the density of the liquid.

Boundary Conditions

In order to solve the set of coupled differential Eqs. (6), (7), (8), and (9), the values of R, x_f, a_p, c_p, and c_f at the foam–liquid interface should be specified. The liquid holdup at the foam–liquid interface can be set equal to the void fraction for closed packed sphere (*18*), i.e.,

$$\epsilon_0 = 0.26 \tag{18}$$

Since the liquid holdup at the top of the foam column is usually much smaller than 0.26 as a result of drainage, the flow rate at the top of the foam column is much smaller than the rate of entrainment of liquid at the foam–liquid interface. A material balance of liquid around the foam therefore yields

$$\frac{G\epsilon_0}{1 - \epsilon_0} = \frac{4}{15} N_0 n_p a_{p_0} u R_0 \tag{19}$$

The superficial gas velocity G is known and the initial bubble size R_0 depends on the type of sparger used. Equations (18) and (19) can be solved for x_{f_0} and a_{p_0} by recognizing that

$$\epsilon_0 = N_0 n_f A_f x_{f_0} + N_0 n_p a_{p_0} l_0 \tag{20}$$

The surfactant concentration in the plateau border c_{p_0} and thin films c_{f_0} at the foam–liquid interface can be taken to be equal to the pool concentration c_B, i.e.,

$$c_{f_0} = c_B, \qquad c_{p_0} = c_B \tag{21}$$

The pool concentration should satisfy the overall mass balance for the surfactant given by

$$Fc_F = Bc_B + Tc_T \tag{22}$$

where B and T refer to the bottom and top product flow rates expressed per unit cross-sectional area of the column. Combining Eq. (22) with the overall material balance

$$F = B + T \tag{23}$$

one obtains

$$c_B = \frac{F}{(F - T)}c_F - \frac{T}{(F - T)}c_T \tag{24}$$

Since T and c_T depend on the unknown ϵ_T, c_{fT}, and c_{pT}, c_B is not known *a priori*. Consequently, a trial and error procedure has to be employed, i.e., Eqs. (6)–(9) have to be solved with bounding conditions (18)–(21) for an assumed c_B in order to obtain ϵ_T, c_{fT}, and c_{pT}. Based on these calculated values, c_B is to be evaluated using Eq. (24) and compared with the assumed value. If these two do not agree, the same procedure is to be repeated until the two successive values agree within the specified tolerance.

ADSORPTION ISOTHERM OF NONIONIC SURFACTANTS AT THE AIR–WATER INTERFACE

The adsorption isotherms of alkanols (C_3–C_{10}) at the air–water interface are given by (*19*)

$$c = \frac{\Gamma_\infty R_g T}{18K_p} \frac{\Gamma^*}{1 - \Gamma^*} \exp\left[-\frac{2H^s}{R_g T}\Gamma^* \right] \tag{25}$$

where $\Gamma^* = \Gamma/\Gamma_\infty$, Γ is the surface concentration, Γ_∞ is the saturation surface concentration, R_g is the gas constant, T is the temperature, K_p is a constant, and H^s is the partial molar free energy of surface mixing at infinite dilution. The equation of state for alkanols is given by (*19*)

$$\Pi = -R_g T\Gamma_\infty\left[\ln (1 - \Gamma^*) + \frac{H^s}{R_g T}\Gamma^{*2}\right] \tag{26}$$

RESULTS AND DISCUSSION

Equations (6)–(9) were solved with boundary conditions (18)–(21) for different coalescence frequencies and mixing parameters in order to investigate the effect of coalescence on enrichment and recovery at different superficial gas velocities, bubble sizes, and inlet concentrations. All the calculations were performed for the nonanol–water system. The values of the parameters K_p, Γ_∞, and H^s in Eqs. (25) and (26) can be found elsewhere (*13*). The three models of coalescence frequencies considered are

$$\beta = a \tag{27}$$

$$\beta = bR \tag{28}$$

and

$$\beta = cR^2 \tag{29}$$

where a, b, and c are constants. Most of the calculations to investigate the effect of coalescence at different operating conditions were performed for the case of constant coalescence frequency. Typical profiles of bubble size R, number of bubbles per unit volume N, and liquid holdup ϵ along the length of the foam column for two different coalescence frequencies are shown in Fig. 1. As expected, the bubble size increases because of coalescence, this increase being more pronounced at higher coalescence frequencies. Conversely, the number of bubbles per unit volume decreases with foam height as a result of coalescence (Fig. 1). The liquid holdup decreases dramatically near the foam–liquid interface as a result of large rates of film and plateau border drainage and is independent of coalescence frequency (Fig. 1). The subsequent decrease in the liquid holdup is not significant for small coalescence frequency. For larger coalescence frequency, however, the liquid holdup decreases significantly with foam height. Such a behavior can be attributed to the increase in the rate of liquid drainage for larger bubble sizes. Consequently, the significant decrease in the liquid holdup for larger coalescence frequencies is a result of increased rates of liquid drainage due to larger bubble sizes.

The effects of coalescence on enrichment and recovery for two different inlet bubble sizes are shown in Fig. 2. In a foam column, coalescence leads to (a) an increase in the surfactant concentration due to internal reflux with subsequent increase in the surface concentration, (b) a decrease in the liquid holdup because of increased liquid drainage rates as a result of larger bubble sizes, and (c) a decrease in the surface area because of larger bubble sizes. The first two effects lead to an increase in the enrichment whereas the last two effects lead to lower recoveries. The second effect of coalescence seems to be predominant since coalescence leads to higher enrichment and lower recovery, as can be seen from Fig. 2. Since liquid drainage is faster for larger bubbles, larger bubbles lead to higher enrichments and lower recoveries (Fig. 2). Moreover, the bubble size increases more rapidly with coalescence frequency for larger bubbles than for smaller

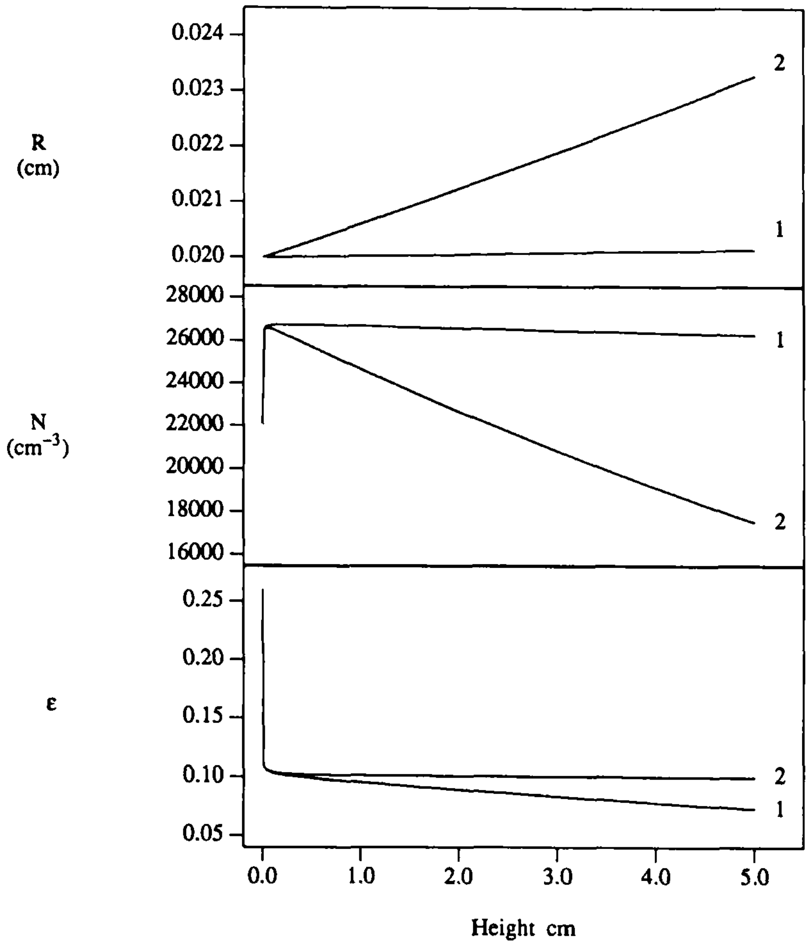

FIG. 1. Change in bubble radius (R), number of bubbles per unit volume (N), and liquid holdup (ϵ) along the height of the foam column for two dimensionless coalescence frequencies. For Curve 1, $\beta\theta = 0.05$, and for Curve 2, $\beta\theta = 1.0$, bubble radius at the foam–liquid interface, $R_0 = 0.02$ cm, $G = 0.02$ cm/s, inlet nonanol concentration $c_F = 8 \times 10^{-8}$ g·mol/cm^3, and feed flow rate $F = 6 \times 10^{-2}$ cm^3/cm^2·s.

bubbles, thus resulting in stronger dependence of enrichment and recovery on coalescence for larger bubbles.

The effect of coalescence on enrichment and recovery for two different gas velocities is shown in Fig. 3. As expected, enrichment decreases and recovery increases at a higher gas velocity because of larger liquid holdups resulting from more entrainment of liquid. The effect of coalescence on

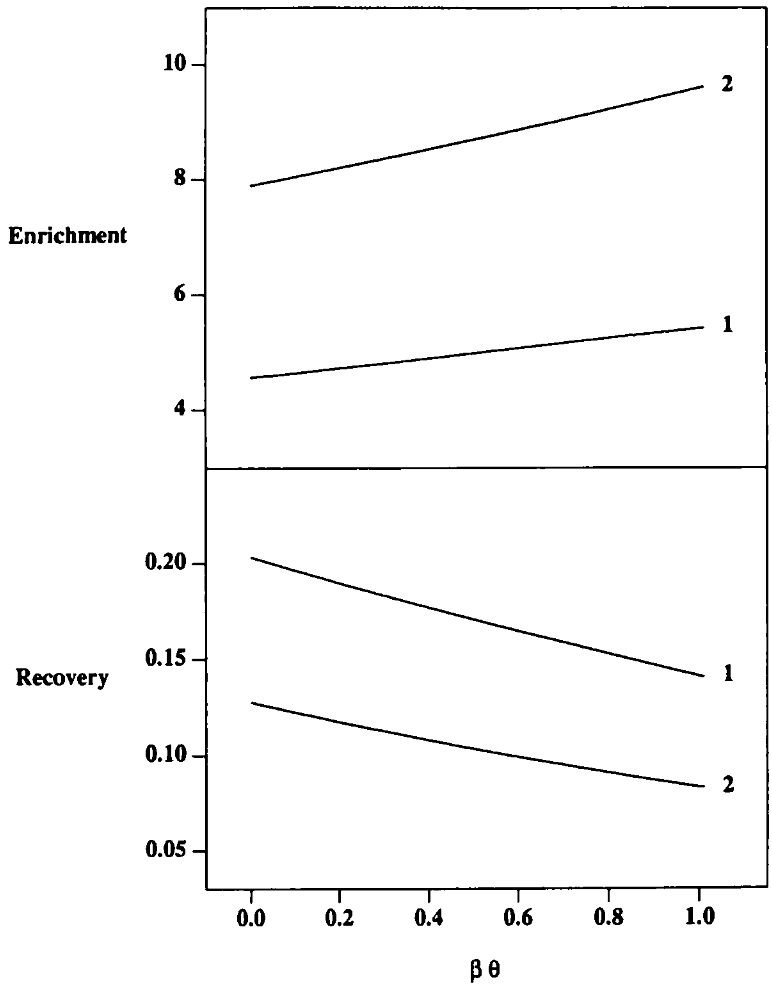

FIG. 2. Effect of dimensionless coalescence frequency βθ on enrichment and recovery for different inlet bubble sizes. Inlet bubble size for Curve 1 is 0.01 cm and for Curve 2 is 0.015 cm; G = 0.01 cm/s, $c_F = 8 \times 10^{-8}$ g·mol/cm^3, $F = 6 \times 10^{-2}$ cm^3/cm^2·s, and foam height is 5 cm.

enrichment and recovery for different inlet nonanol concentrations is shown in Fig. 4. At lower inlet concentrations, an increase in the inlet concentration would result in an increase in the surface concentration and therefore a decrease in the surface tension. The former effect tends to increase the enrichment whereas the latter effect results in lower rates of drainage, thus leading to lower enrichment. The former effect seems to be predom-

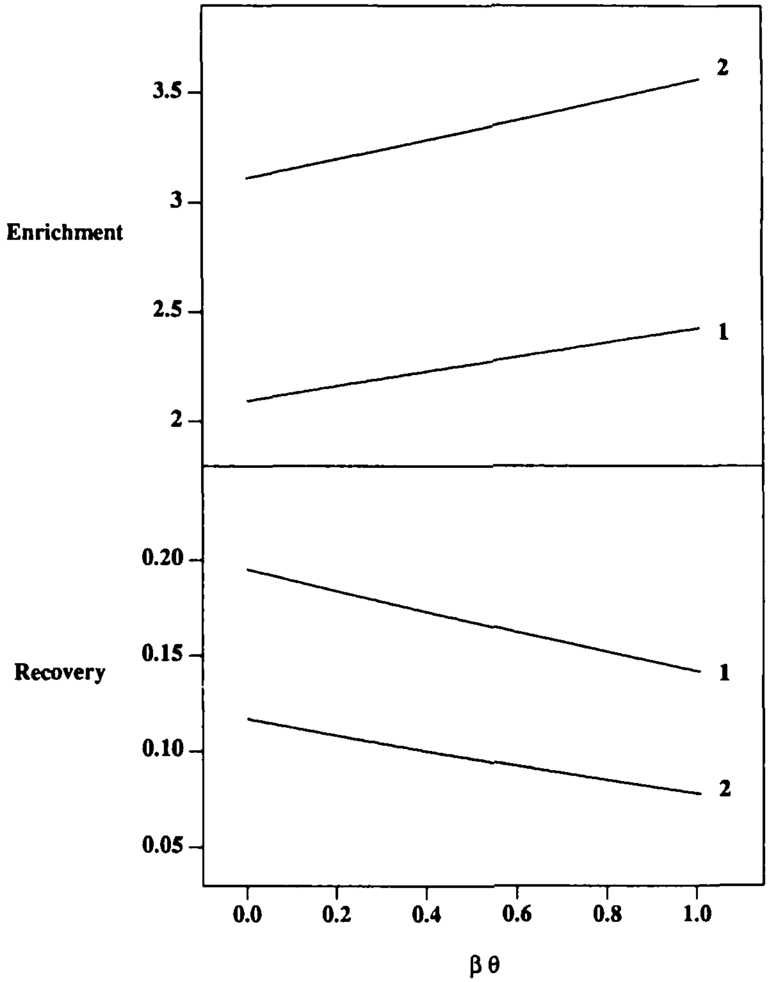

FIG. 3. Effect of dimensionless coalescence frequency βθ on enrichment and recovery at two superficial gas velocities. For Curve 1, G = 0.03 cm/s, and for Curve 2, G = 0.02 cm/s; R = 0.02 cm, $c_F = 4 \times 10^{-8}$ g·mol/cm^3, $F = 6 \times 10^{-2}$ cm^3/cm^2·s, and foam height is 5 cm.

inant since enrichment is found to increase with concentration at lower inlet concentrations. At higher concentrations, however, because of the fact that surface concentrations and surface pressure plateau to constant values, the relative contribution of the surfactant adsorbed at the interface compared to that in the bulk decreases with an increase in the inlet concentrations. Consequently, enrichment decreases with concentration at

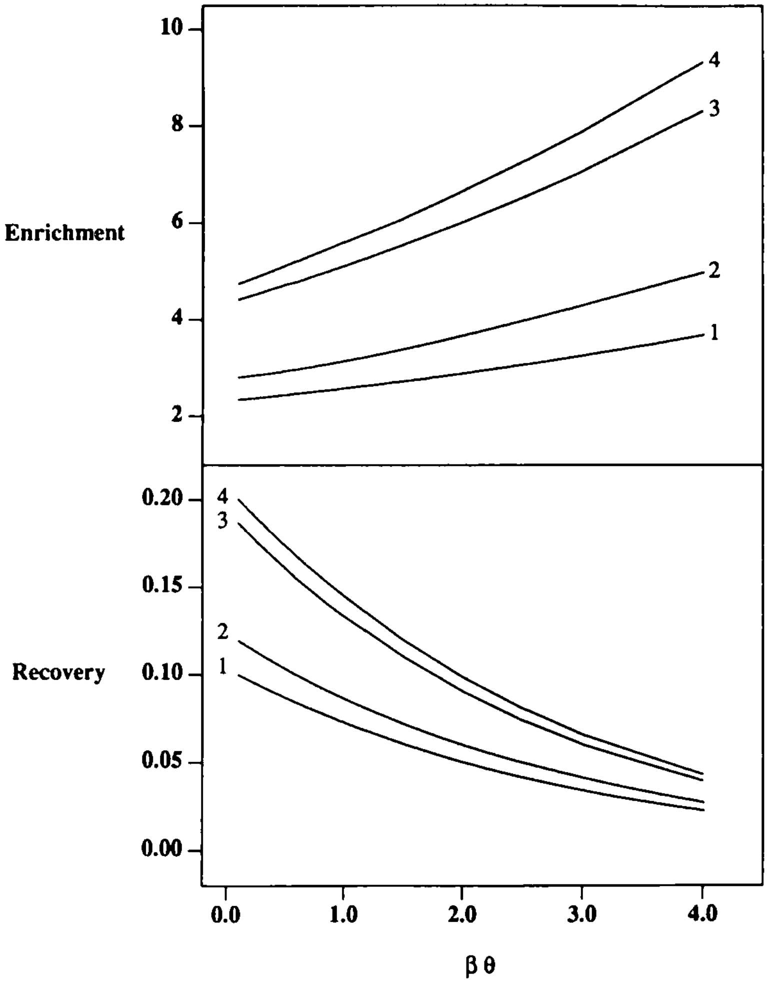

FIG. 4. Effect of dimensionless coalescence frequency $\beta\theta$ on enrichment and recovery for different inlet feed concentrations. For Curve 1, $c_F = 2 \times 10^{-8}$; Curve 2, $c_F = 4 \times 10^{-8}$; Curve 3, $c_F = 9.0 \times 10^{-8}$; and Curve 4, $c_F = 7.5 \times 10^{-8}$ g·mol/cm^3; $R = 0.01$ cm, $G = 0.01$ cm/s, $F = 6 \times 10^{-2}$ cm^3/cm^2·s, and foam height is 5 cm.

higher inlet concentrations. Therefore, there exists an optimum inlet concentration at which enrichment and recovery are maximum. This is shown in Fig. 5.

Comparison of the predicted enrichment and recovery for three different models are shown in Fig. 6 where the enrichment and recovery are plotted for different values of $\beta_0\theta$, β_0 being the coalescence frequency correspond-

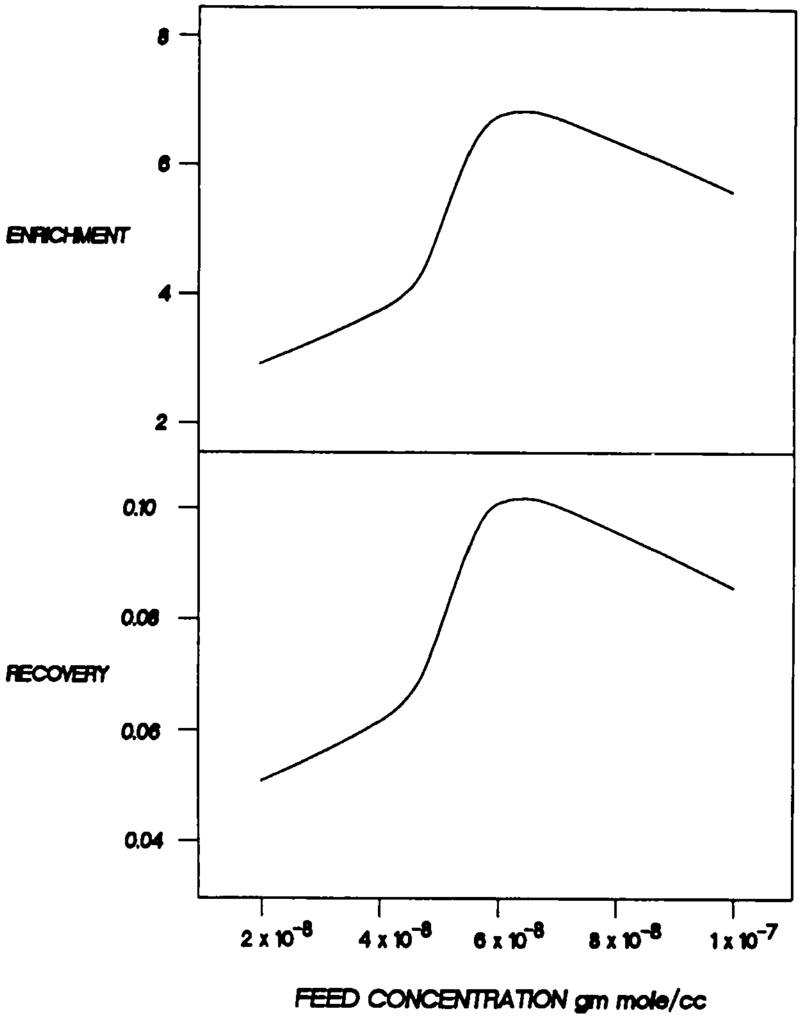

FIG. 5. Effect of inlet feed concentration on enrichment and recovery of nonanol; $R = 0.01$ cm, $G = 0.01$ cm/s, $\beta\theta = 2.0$, $F = 6 \times 10^{-2}$ cm^3/cm^2·s, and foam height is 5 cm.

ing to the inlet bubble size. Enrichment is the highest and recovery lowest for the model in which $\beta \propto R^2$. Enrichments were found to decrease in the order $\beta \propto R^2 > \beta \propto R > \beta = \beta_0$. Such a behavior is to be expected since the coalescence frequency decreases in the same order. At very low coalescence frequencies, however, there was very little difference in the enrichments and recoveries predicted by the models. An increase in the

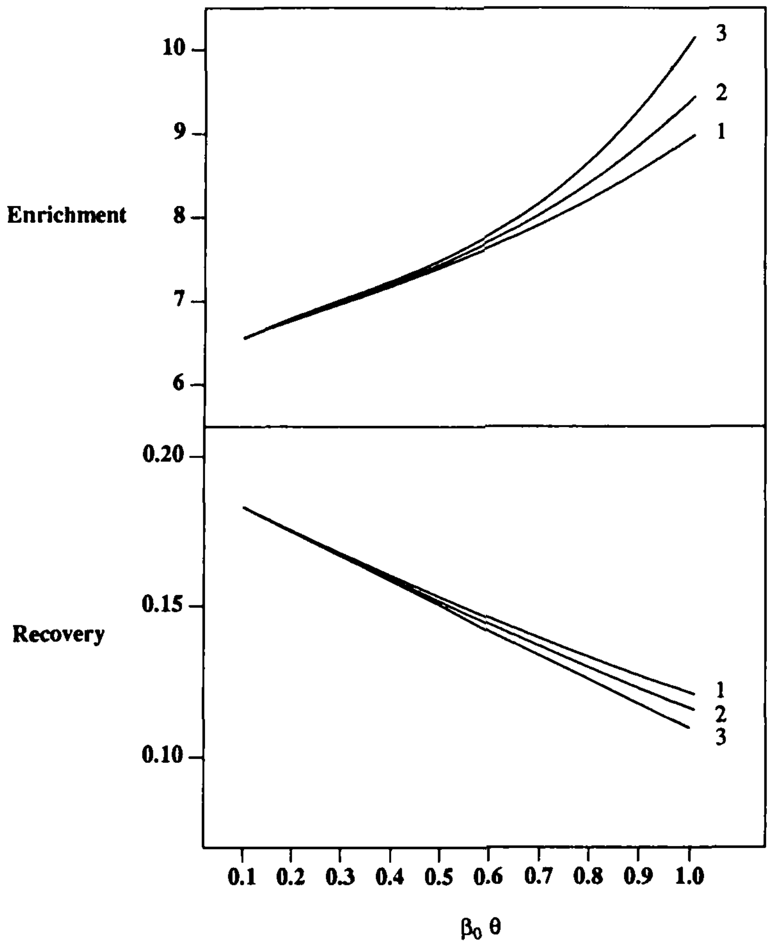

FIG. 6. Comparison of predicted enrichment and recovery for three models of coalescence frequency. Curve 1 refers to the case where β = constant; for Curve 2, $\beta \propto R$; and for Curve 3, $\beta \propto R^2$.

mixing parameter m should result in higher surfactant concentration in the film because of better mixing of the liquid between plateau borders and films and therefore to higher surface concentration of nonanol. Consequently, an increase in m should lead to higher enrichments and recoveries. For the conditions for which the effect of m was studied, there was only a marginal increment in the surface concentration of nonanol at the film interface at higher values of m and therefore enrichment and recovery did not increase significantly with an increase in the mixing parameter.

CONCLUSIONS

A model for the hydrodynamics of a coalescing foam bed is proposed. Foam bed is assumed to consist of dodecahedral bubbles of the same size at any cross section even though bubble size increases with foam height because of coalescence. The model accounts for the drainage of liquid from thin films to the neighboring plateau borders due to plateau border suction as well as drainage of liquid through interconnected network of plateau borders due to gravity in the evaluation of liquid holdup profile in the foam bed. Partial mixing of the liquid in thin films and plateau borders due to internal reflux resulting from coalescence is accounted for in the present model. This model was employed to calculate enrichment and recovery in a continuous foam fractionation column for the nonanol–water system for three different phenomenological models for coalescence frequency. Even though liquid holdup decreased dramatically near the foam–liquid interface because of rapid liquid drainage, it more or less remained constant with foam height for small coalescence frequencies sufficiently away from the interface. For large coalescence frequencies, however, liquid holdup decreased significantly with foam height as a result of increased liquid drainage due to larger bubble sizes. Larger bubble sizes and lower superficial gas velocities were found to result in higher enrichments and lower recoveries. There exists an optimum inlet concentration for which enrichment was found to be maximum. Comparison of enrichments and recoveries for different models for coalescence frequencies indicated that enrichment decreased and recovery increased in the order $\beta \propto R^2 > \beta \propto R > \beta = \beta_0$. The effect of mixing parameter on enrichment and recovery was found to be insignificant.

REFERENCES

1. R. Lemlich, in *Progress in Separation and Purification*, Vol. 1 (E. S. Perry, ed.), Wiley-Interscience, New York, 1968.
2. Y. Okamoto and E. J. Chou, "Foam Separation Processes," in *Handbook of Separation Techniques for Chemical Engineers* (P. A. Schweitzer, ed.), Wiley, New York, 1979.
3. P. Somasundaram and K. P. Ananthapadmanabhan, "Bubble and Foam Separations—Ore Floatation," in *Handbook of Separation Process Technology* (R. W. Rousseau, ed.), Wiley, New York, 1987.
4. D. J. Wilson and A. N. Clark, "Bubble and Foam Separations—Waste Management," in *Handbook of Separation Process Technology* (R. W. Rousseau, ed.), Wiley, New York, 1987.
5. G. D. Miles, L. Shedlovsky, and J. Ross, *J. Phys. Chem.*, *49*, 3 (1945).
6. W. M. Jacobi, K. E. Woodcock, and C. S. Grove, *Ind. Eng. Chem.*, *48*, 2046 (1956).
7. L. Steiner, R. Hunkeler, and S. Hartland, *Trans. Inst. Chem. Eng.*, *55*, 153 (1977).
8. S. Hartland and A. D. Barber, *Ibid.*, *52*, 43 (1974).
9. D. Desai and R. Kumar, *Chem. Eng. Sci.*, *38*, 1525 (1983).
10. D. Desai and R. Kumar, *Chem. Eng. Sci.*, *39*, 1559 (1984).

11. R. A. Leonard and R. Lemlich, *AIChE J.*, *11*, 18 (1965).
12. P. A. Haas and H. F. Johnson, *Ind. Eng. Chem., Fundam.*, *6*, 225 (1967).
13. G. Narsimhan and E. Ruckenstein, *Langmuir*, *2*, 230 (1986).
14. R. Lemlich, *Ind. Eng. Chem., Fundam.*, *17*, 89 (1978).
15. G. Narsimhan and E. Ruckenstein, *Langmuir*, *2*, 494 (1986).
16. L. Brown, G. Narsimhan, and P. C. Wankat, *Biotechnol. Bioeng.*, *36*, 947 (1990).
17. I. B. Ivanov and D. S. Dimitrov, *Colloid Polym. Sci.*, *252*, 982 (1974).
18. D. Desai and R. Kumar, *Chem. Eng. Sci.*, *37*, 1361 (1982).
19. E. H. Lucassen-Reynders, *Prog. Surf. Sci.*, *10*, 253 (1976).

Received by editor June 17, 1991